

# THE PHYSICAL REVIEW

*A journal of experimental and theoretical physics established by E. L. Nichols in 1893*

SECOND SERIES, VOL. 170, No. 4

20 JUNE 1968

## $(\alpha, \text{Li})$ Reactions on $\text{B}^{11}$ , $\text{N}^{15}$ , and $\text{F}^{19}\dagger$

P. F. MIZERA\* AND J. B. GERHART

*Department of Physics, University of Washington, Seattle, Washington*

(Received 31 August 1967; revised manuscript received 21 February 1968)

Differential cross sections for  $(\alpha, \text{Li}^7)$  and  $(\alpha, \text{Li}^{7*} 0.478)$  reactions have been measured on  $\text{B}^{11}$  to the ground state of  $\text{Be}^8$ , on  $\text{N}^{15}$  to the ground and first excited states of  $\text{C}^{12}$ , and on  $\text{F}^{19}$  to the ground state of  $\text{O}^{16}$ , using 42-MeV  $\alpha$  particles. In addition, the  $(\alpha, \text{Li}^6)$  reaction was studied on  $\text{N}^{15}$ , leading to the ground state of  $\text{C}^{13}$  and on  $\text{F}^{19}$ , leading to the ground and first excited states of  $\text{O}^{17}$ . A zero-range distorted-wave Born-approximation (DWBA) code was used to fit the  $(\alpha, \text{Li}^7)$  angular distributions assuming a one-step pickup mechanism. Triton reduced widths are extracted from the DWBA calculations normalized to the experimental differential cross sections, and then compared with approximate shell-model calculations. The comparison between the extracted and calculated reduced widths shows that  $\text{B}^{11}$ ,  $\text{N}^{15}$ , and  $\text{F}^{19}$  are probably consistent with a single-particle interpretation, although a small enhancement for triton clustering is observed for the ground state of  $\text{F}^{19}$ .

### I. INTRODUCTION

ALTHOUGH single-nucleon pickup reactions have been studied extensively both experimentally and theoretically, less work on multinucleon transfers has been completed and the mechanism for these reactions is poorly understood. Some recent experiments using deuterons as projectiles have been interpreted with limited success as transfers of  $\alpha$  particles<sup>1,2</sup> or heavier clusters.<sup>3</sup> Another case has been analyzed as an indirect reaction<sup>4</sup> because of fluctuations in the angular distributions with incident energy. However, for some  $(p, \alpha)$  reactions, direct processes have been assumed to give rise to similar fluctuations.<sup>5</sup> If the  $(\alpha, \text{Li}^7)$  reactions can be interpreted as a triton pickup reaction, neglecting other competing direct processes, these results might help clarify the interpretation of the  $(p, \alpha)$  reaction mechanism. The experiments on  $(\alpha, \text{Li}^7)$  reactions reported here were carried out with this in mind.

Because the ground state of  $\text{F}^{19}$  has been predicted to have a large contribution of triton plus  $\text{O}^{16}$  ground-state core configuration,<sup>6</sup> it was used as one of the targets studied here.  $\text{N}^{15}$  and  $\text{B}^{11}$  were investigated for comparison with the  $\text{F}^{19}$  results. Also, angular distributions for the  $(\alpha, \text{Li}^6)$  reaction on  $\text{F}^{19}$  and  $\text{N}^{15}$  were obtained.

Angular distributions for the  $(\alpha, \text{Li}^7)$  reactions were fit by a DWBA code,<sup>7</sup> assuming a one-step pickup mechanism. The extracted reduced widths are compared with a set calculated using the nuclear shell model in order to reveal possible cluster effects. The DWBA analysis of the  $(\alpha, \text{Li}^6)$  reaction was not as successful as for the  $\text{Li}^7$  transitions and is not presented here.

### II. EXPERIMENTAL PROCEDURE

A beam of 42-MeV  $\alpha$  particles from the University of Washington 60-in. cyclotron was used throughout this investigation. A description of the external beam system has been given previously.<sup>8</sup> The energy spread of the analyzed  $\alpha$  beam at the center of a 60-in. scatter-

<sup>†</sup> Supported in part by the U. S. Atomic Energy Commission. A preliminary account of this work was given in P. F. Mizera, F. W. Slee, and J. B. Gerhart, *Bull. Am. Phys. Soc.* **11**, 316 (1966).

\* Present address: at Aerospace Corp., El Segundo, Calif.

<sup>1</sup> L. J. Denes, W. W. Daehnick, and R. M. Drisko, *Phys. Rev.* **148**, 1097 (1966).

<sup>2</sup> F. W. Slee, Ph.D. thesis, University of Washington, 1966 (unpublished).

<sup>3</sup> L. J. Denes and W. W. Daehnick, *Phys. Rev.* **154**, 928 (1967).

<sup>4</sup> R. E. Brown, J. S. Blair, D. Bodansky, N. Cue, and C. D. Kavaloski, *Phys. Rev.* **138**, B1394 (1965).

<sup>5</sup> K. L. Walsh and S. Edwards, *Nucl. Phys.* **65**, 382 (1965).

<sup>6</sup> R. K. Sheline and K. Wildermuth, *Nucl. Phys.* **21**, 196 (1960).

<sup>7</sup> R. H. Bassel, R. M. Drisko, and G. R. Satchler, Oak Ridge National Laboratory Report No. ORNL-3248, 1962 (unpublished).

<sup>8</sup> A. J. Lieber, F. H. Schmidt, and J. B. Gerhart, *Phys. Rev.* **126**, 1496 (1962).

ing chamber used for this study is estimated to be less than 100 keV.

Lithium particles were observed with a detector telescope consisting of a 25- $\mu$ -thick solid-state transmission detector used as a  $\Delta E$  counter and a solid-state  $E$  detector thick enough to stop all lithium particles from the reactions studied.

Pulses from two charge-sensitive preamplifiers were split, one branch going to a particle identification system and the other to a pulse adder and then to a 512-channel analyzer.  $\Delta E$  and  $E$  pulses were sent through a two-channel linear gate into a pulse multiplier<sup>9</sup> to obtain a constant output corresponding to lithium ions which was used to gate the 512-channel analyzer. Figure 1 shows an oscilloscope display of the multiplier output plotted as a function of the total energy. This illustrates the separation of  $\text{Li}^6$  and  $\text{Li}^7$  events, shown at the center of the display, which was achieved with this system. The energy calibration for the lithium ions was obtained by measuring knockout lithiums from a  $\text{LiF}$  target at various angles.

The boron targets were self-supporting foils of 98.6% isotopically pure  $\text{B}^{11}$ . The  $\text{N}^{15}$  and  $\text{F}^{19}$  targets were vacuum-evaporated on thin carbon foils. The compounds used were KCN (95.5% isotopically enriched  $\text{N}^{15}$ ) and  $\text{CaF}_2$ . All targets were between 100–300  $\mu\text{g}/\text{cm}^2$  thick. The uncertainties of measurements of target thicknesses, obtained by various methods, corresponded to uncertainties in the absolute cross section (less than 14% in all cases).

The errors shown for the experimental points presented in later sections include statistical errors and in some cases uncertainties arising from the separation of partly overlapping peaks in the pulse-height distributions. Each angular distribution was repeated at least twice. The final values are the weighted averages

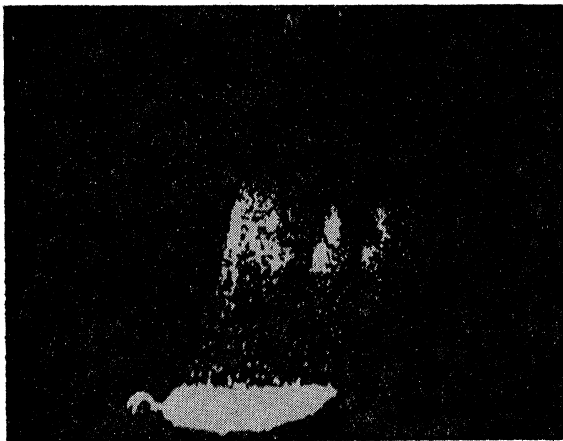


FIG. 1. Photograph showing the multiplier output  $\Delta E(E+k_1\Delta E+k_2)$  along the vertical axis plotted as a function of the total energy  $E+\Delta E$  along the horizontal axis. Lithium ions are in the center of the picture,  $\text{Li}^7$  lying higher than  $\text{Li}^6$ .

<sup>9</sup> V. Radeka, IEEE Trans. Nucl. Sci. NS-11, 302 (1964).

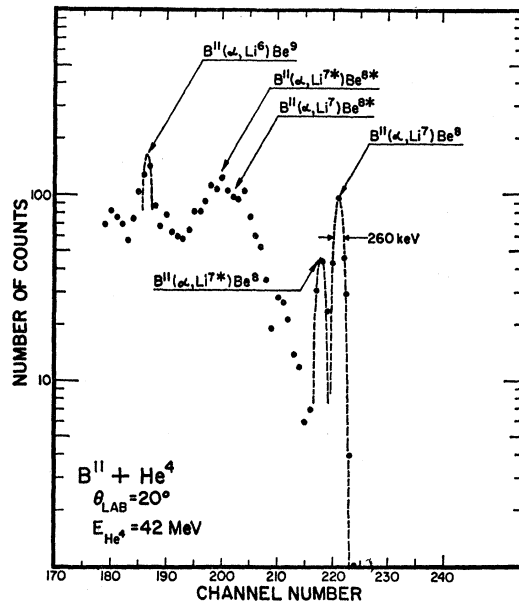


FIG. 2. Pulse-height spectrum for lithium ions at  $20^\circ$  in the laboratory system from 42-MeV  $\alpha$  particles incident on  $\text{B}^{11}$ .

of the different measurements. In addition, selected points of the angular distributions were repeated at beam energies reduced by 0.6 and 1.2 MeV. No noticeable fluctuations of the differential cross sections with incident energy were observed.

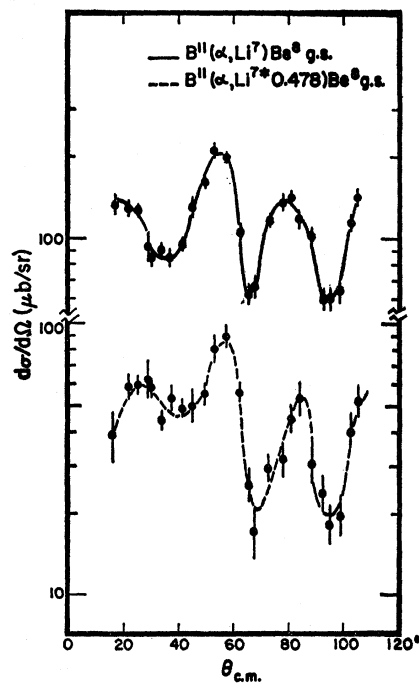


FIG. 3. Angular distributions for  $\text{B}^{11}(\alpha, \text{Li}^7)\text{Be}^9$  and  $\text{B}^{11}(\alpha, \text{Li}^{7*})\text{Be}^9$ . The solid and dashed curves are meant as visual guides.

## III. EXPERIMENTAL RESULTS

Figure 2 shows a pulse-height spectrum for lithium ions at a laboratory angle of  $20^\circ$  resulting from the bombardment of  $\text{B}^{11}$  by 42-MeV  $\alpha$  particles. The only transitions analyzed were those to the ground state of  $\text{Be}^8$  because the large decay width of the first excited state of  $\text{Be}^8$  obscured other peaks in the spectrum. Angular distributions for the  $\text{Li}^7$  ground- and  $\text{Li}^7$  first-excited-state transitions to the ground state of  $\text{Be}^8$  are shown in Fig. 3. Observations were confined to the range from  $10^\circ$  to  $70^\circ$  in the laboratory system. These limits were set by Rutherford scattering for small angles and by the detector telescope energy threshold for large angles.

A pulse-height spectrum for  $\text{N}^{15}$  at a laboratory angle of  $40^\circ$  is shown in Fig. 4.  $\text{Li}^7$  ground- and first-excited-state transitions to the ground and first excited states of  $\text{C}^{12}$  were studied. In addition, the  $\text{N}^{15}(\alpha, \text{Li}^6)\text{C}^{13}(\text{g.s.})$  reaction was also analyzed. The  $\text{Li}^7$  angular distributions are shown in Figs. 5 and 6.

Figure 7 shows the pulse-height spectrum of lithium ions emerging from  $\text{F}^{19}$  at a laboratory angle of  $25^\circ$ . The four reactions analyzed were the  $\text{Li}^7$  ground- and first-excited-state transitions leading to the ground state of  $\text{O}^{16}$ , and the  $\text{Li}^6$  reaction proceeding to the ground and first excited states of  $\text{O}^{17}$ . The peaks corresponding to higher transitions were impossible to separate from each other.  $\text{Li}^7$  angular distributions are shown in Fig. 8. Angular distributions of the  $\text{Li}^6$  transitions to the ground states of  $\text{C}^{13}$ ,  $\text{O}^{17}$ , and the first excited state of  $\text{O}^{17}$  are shown in Fig. 9.

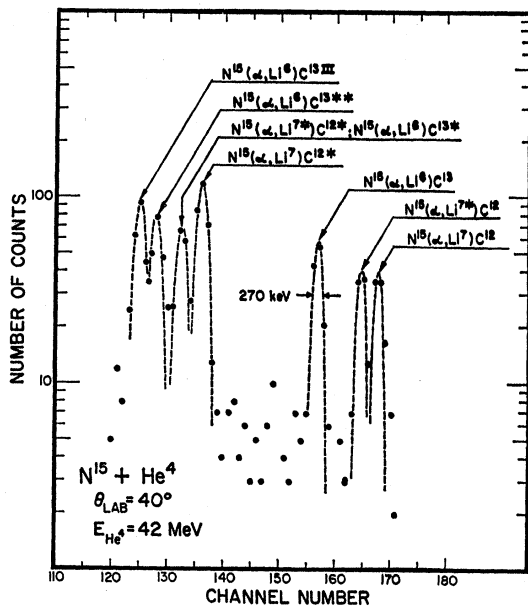


FIG. 4. Pulse-height spectrum for lithium ions at  $40^\circ$  in the laboratory system from 42-MeV  $\alpha$  particles incident on  $\text{N}^{15}$ .

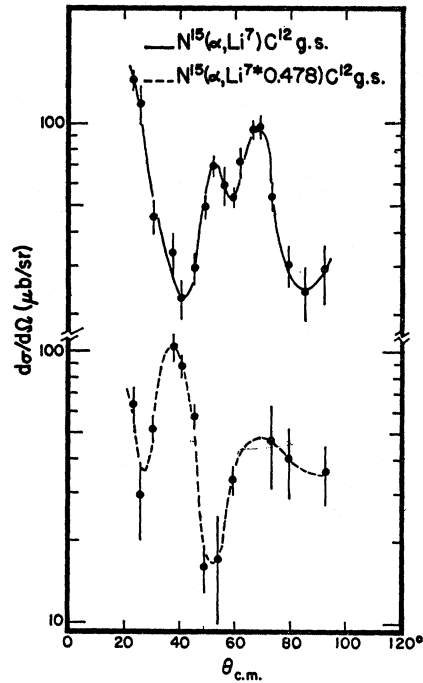


FIG. 5. Angular distribution for  $\text{N}^{15}(\alpha, \text{Li}^7)\text{C}^{12}$  and  $\text{N}^{15}(\alpha, \text{Li}^{7*})\text{C}^{12}$ . The solid and dashed curves are meant as visual guides.

## IV. DWBA CALCULATIONS

An attempt was made to fit the  $(\alpha, \text{Li}^7)$  reactions using the DWBA code, T-SALLY,<sup>7</sup> assuming a one-step

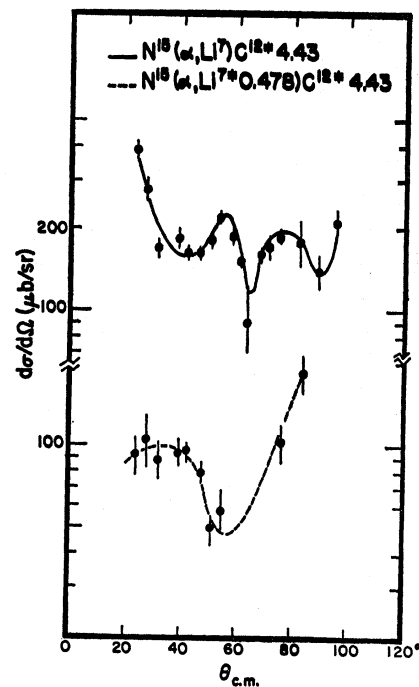


FIG. 6. Angular distributions for  $\text{N}^{15}(\alpha, \text{Li}^7)\text{C}^{12*}$  and  $\text{N}^{15}(\alpha, \text{Li}^{7*})\text{C}^{12*}$ . The solid and dashed curves are meant as visual guides.

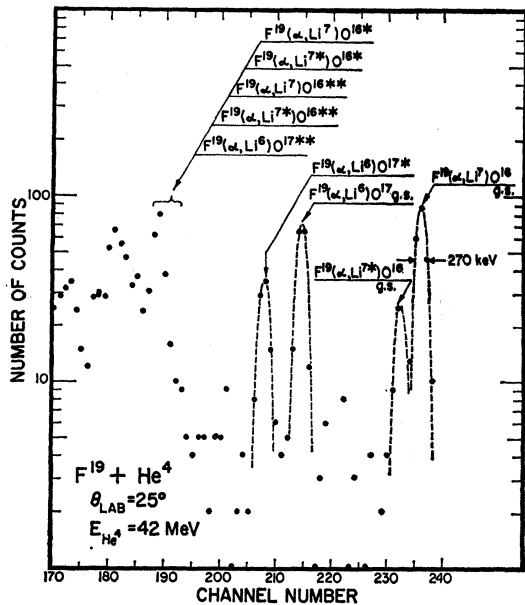


FIG. 7. Pulse-height spectrum for lithium ions at  $25^\circ$  in the laboratory system from 42-MeV  $\alpha$  particles incident on  $F^{19}$ .

cluster pickup mechanism. Some of the assumptions made to describe these multinucleon transfer reactions in a form suitable for the DWBA calculations have been discussed by Denes, Daehnick, and Drisko.<sup>1</sup> The inherent problems arising from the use of a zero-range code will be discussed in Sec. VI.

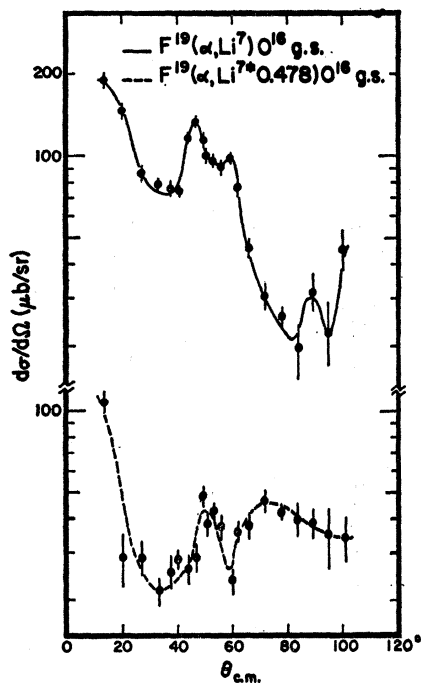


FIG. 8. Angular distributions for  $F^{19}(\alpha, Li^7)O^{16}$  and  $F^{19}(\alpha, Li^{7*})O^{16}$ . The solid and dashed curves are meant as visual guides.

The real and imaginary optical potentials used for the initial channel were of the Woods-Saxon volume form

$$V(r) = -V\{1 + \exp[(r - r_0 A^{1/3})/a]\}^{-1}.$$

The same radius and diffuseness were used for both the imaginary and the real potentials. The real part of the potential used for the final channel was also of the volume form while the imaginary part was of the surface Gaussian form

$$W(r) = -W \exp\{-[(r - r_0' A^{1/3})/a']^2\}.$$

The Coulomb potential used was that of a uniformly charged sphere of radius  $R_c = r_c A^{1/3}$  for both the initial and final channels.

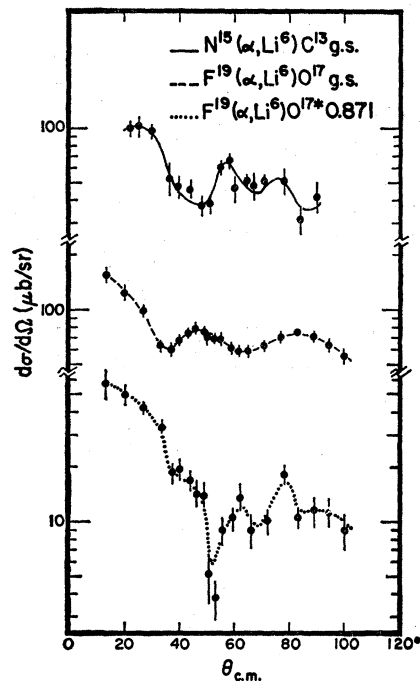


FIG. 9. Angular distributions for  $N^{15}(\alpha, Li^6)C^{13}$ ,  $F^{19}(\alpha, Li^6)O^{17}$ , and  $F^{19}(\alpha, Li^6)O^{17*}$ . The curves are meant as visual guides.

Optical-model parameters for the incident  $\alpha$  particles in  $B^{11}(\alpha, Li^7)Be^8$  were obtained by visually fitting the experimental angular distribution<sup>10</sup> for elastic scattering of 42-MeV  $\alpha$  particles from  $C^{12}$ . For  $N^{15}(\alpha, Li^7)C^{12}$ , averages of the incident particle parameters similarly obtained from data<sup>11</sup> for 42-MeV  $\alpha$ -particle elastic scattering from  $N^{14}$  and  $O^{16}$  were used. For  $F^{19}(\alpha, Li^7)O^{16}$ , the incident-particle parameters were obtained from data<sup>12</sup> for 42-MeV  $\alpha$ -particle elastic scattering from

<sup>10</sup> I. Naqib, Ph.D. thesis, University of Washington, 1962 (unpublished).

<sup>11</sup> A. I. Yavin and G. W. Farwell, Nucl. Phys. **12**, 1 (1959).

<sup>12</sup> D. C. Shreve, Nuclear Physics Laboratory, University of Washington (private communication).

Ne<sup>20</sup>. The values of the incident particle optical parameters are listed in Table I.

The form factor in the DWBA calculations uses the bound-state wave function of the picked-up cluster with quantum numbers chosen to conserve both internal energy and angular momentum in the target nucleus. The quantum numbers used for the Li<sup>7</sup> transitions to the ground states of Be<sup>8</sup> and C<sup>12</sup> were  $N=2$  and  $L=1$ . These quantum numbers are associated with the center-of-mass wave function of the three nucleons. The internal wave function of these nucleons is assumed to be that corresponding to the ground state of a triton, or 1s. The cluster wave functions are also assumed to have the same form as those of the single-particle wave func-

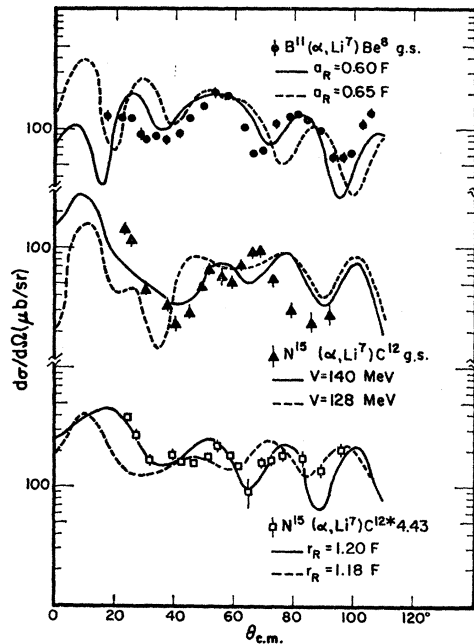


FIG. 10. Examples of the DWBA fits to the experimental data. The dashed curves show the results of using average Li<sup>7</sup> parameters while the solid curves show the DWBA fits after changing the parameters as shown in the figure.

tions. These assumptions have been discussed by Wildermuth and Kanellopoulos.<sup>13</sup> Both  $2P$  and  $1F$  bound-state wave functions were used for the Li<sup>7</sup> transitions to the first excited state of C<sup>12</sup>, and were needed to give a reasonable fit to the data. The magnitude of the  $1F$  contribution was twice that of the  $2P$  contribution for the final analysis. The bound-state wave function used for the Li<sup>7</sup> transition to the ground state of O<sup>16</sup> was  $4S$ . These wave functions are calculated by adjusting the depth of a Woods-Saxon well to yield a specified binding or separation energy of the cluster from the target nucleus. The shape parameters for this well were chosen to be  $r_0=r_c=1.25$  F and  $a=0.5$  F.

<sup>13</sup> K. Wildermuth and Th. Kanellopoulos, Nucl. Phys. 7, 150 (1958); 9, 449 (1958).

TABLE I. Optical-model parameters for the elastic scattering of 42-MeV  $\alpha$  particles.

	B <sup>11</sup>	N <sup>15</sup>	F <sup>19</sup>
$V$ (MeV)	40.0	50.0	50.0
$W$ (MeV)	16.0	14.0	20.0
$r_0$ (F)	1.90	1.60	1.82
$r_c$ (F)	1.90	1.60	1.82
$a$ (F)	0.48	0.65	0.40

Li<sup>7</sup> parameters were obtained initially from Denes, Daehnick, and Drisko<sup>1</sup> by fitting the angular distribution for elastic scattering of 7.3-MeV Li<sup>7</sup> ions from C<sup>12</sup>. Some adjustment of these parameters was felt justified because of the more energetic lithium ions (25 to 33 MeV) resulting from the reactions studied here. The angular distributions were fit by using sets of parameters chosen to best fit the data. An average set of parameters derived from these best-fit parameters was used in the final analysis. In some cases small changes of these parameters were made when obvious discrepancies between the experimental data and the theoretical fit occurred. The final optical-model parameters used to describe the Li<sup>7</sup> elastic scattering are given in Table II.

The adjustments in the average parameters, mentioned above, were a change in  $a$  from 0.65 to 0.60 F for reactions leading to the ground states of Be<sup>8</sup> and C<sup>12</sup>, a change in  $r_0$  from 1.18 to 1.20 F for reactions to the first excited state of C<sup>12</sup>, and a change in  $V$  from 128 to 140 MeV for reactions to the ground and first excited states of C<sup>12</sup>. Figure 10 shows the effects of making these adjustments to the average set of Li<sup>7</sup> parameters.

The final DWBA fits for all of the  $(\alpha, \text{Li}^7)$  reactions analyzed are shown in Figs. 11(a) and 11(b).

## V. DISCUSSION

The ratio between the experimental differential cross sections and the DWBA calculations is assumed to be proportional to the probability of triton clustering in the target nucleus:

$$\sigma_{\text{exp}}(\theta)/\sigma_{\text{DWBA}}(\theta) = [(2s_{\text{Li}}+1)/(2s_{\alpha}+1)]R_{\alpha t}R_{ct},$$

where  $s_{\text{Li}}$  and  $s_{\alpha}$  are the ejectile and projectile spins and the  $R$ 's represent the cluster probabilities commonly called reduced widths.  $R_{\alpha t}$  is proportional to the probability of an  $\alpha$  particle and a triton forming the Li<sup>7</sup>

TABLE II. Optical-model parameters for the elastic scattering of Li<sup>7</sup> ions.

	Be <sup>8</sup>	C <sup>12</sup>	C <sup>12*</sup>	O <sup>16</sup>
$V$ (MeV)	128.0	140.0	140.0	128.0
$W$ (MeV)	4.60	4.60	4.60	4.60
$r_0$ (F)	1.18	1.18	1.20	1.18
$r_c$ (F)	2.00	2.00	2.00	2.00
$a$ (F)	0.60	0.60	0.65	0.65
$r_0'$ (F)	2.10	2.10	2.10	2.10
$a'$ (F)	0.50	0.50	0.50	0.50

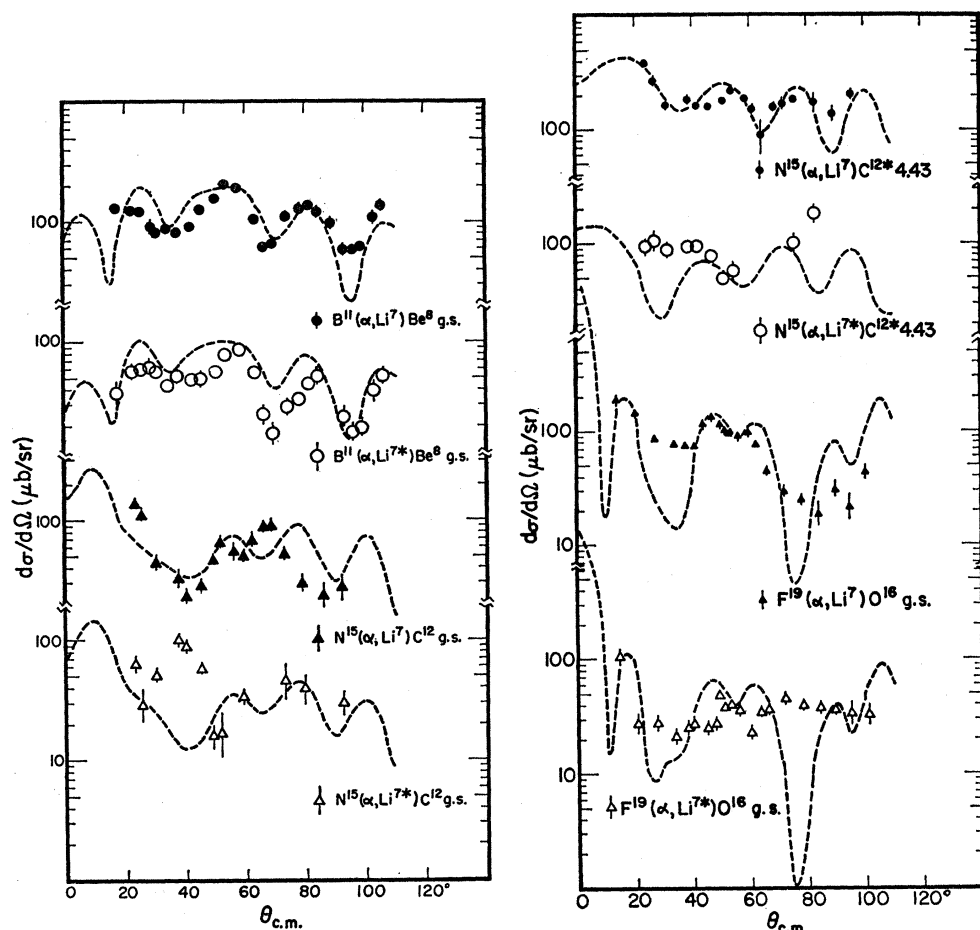


FIG. 11. The dashed curves are the final DWBA fits to the experimental angular distributions.

ejectile and  $R_{ct}$  is proportional to the probability of an inert core and the triton forming the target nucleus.

As can be seen from Fig. 3, the experimental angular distributions for  $B^{11}(\alpha, Li^7)Be^8$  g.s. and  $B^{11}(\alpha, Li^{7*})Be^8$  g.s. are quite similar in shape and differ in magnitude by roughly a factor of 2. This is just the ratio of the spin factors  $(2s_{Li}+1)$  for  $Li^7$  in its ground and first excited states. Since the target reduced widths are the same for these two reactions, this result implies that  $R_{ct}$  is the same for the ground and first excited states of  $Li^7$ . This result agrees well with both cluster and shell-model calculations and was used in the analysis of the data for the other  $Li^7$  transitions. That is, once the DWBA calculation was normalized to the differential cross section for the  $Li^7$  ground-state transition, the

magnitude of the predicted differential cross section for the  $Li^7$  first-excited-state transition was taken to be one-half of the ground-state normalization. The fits shown in Figs. 11(a) and 11(b) illustrate the success of this procedure in all cases.

The normalization factors between the experimental differential cross sections and the DWBA calculations for transitions to the ground state of  $Li^7$  along with the angle at which normalizations were made are given in Table III. The bound-state wave function  $(|t\rangle)_{c.m.}$  used in the DWBA form factor is also listed in Table III.

The normalization factors between the experimental and calculated differential cross sections depend on the angle chosen for making the normalizations. For the cases of the  $B^{11}(\alpha, Li^7)Be^8$ (g.s.), and  $F^{19}(\alpha, Li^7)O^{16}$ (g.s.) reactions, the variations obtained by choosing different angles for normalization were less than 10%. The normalization factors given in Table III fall in the midrange of possible values. For the  $N^{15}(\alpha, Li^7)C^{12}$ (g.s.) reaction, the variations in the normalization factors obtained by choosing different angles were approximately 50%.

For the case of the  $N^{15}(\alpha, Li^7)C^{12*}(4.43)$  reaction, additional variations in the normalization factor are

TABLE III. DWBA normalization for  $A(\alpha, Li^7)B$ .

A	B	$ t\rangle_{c.m.}$	$\theta_N$	$\sigma_{exp}(\theta_N)/\sigma_{DWBA}(\theta_N)$
$B^{11}$	$Be^8$ g.s.	$2p$	$80^\circ$	0.168
$N^{15}$	$C^{12}$ g.s.	$2p$	$50^\circ$	0.094
$N^{15}$	$C^{12*}$	$2p$	$30^\circ$	0.115
		$1f$	$30^\circ$	0.230
$F^{19}$	$O^{16}$ g.s.	$4s$	$20^\circ$	0.225

introduced because of the relative admixture of  $2P$  and  $1F$  wave functions used in the DWBA calculations. As was discussed previously, both contributions were needed to give a reasonable theoretical fit to the data; however, the shape of the theoretical angular distribution was not particularly sensitive to the amount of relative admixture of  $2P$  and  $1F$ . Although the normalization factor pertaining to the individual contributions of  $2P$  or  $1F$  could be varied by almost a factor of 2, the sum of these factors which is proportional to the total triton reduced width was estimated to change less than 5%.

An attempt to calculate theoretically the appropriate reduced widths was made using an approximate method which assumes  $j$ - $j$  coupling and good seniority states. If the shell-model description is valid for the nuclei of interest, we can first represent the target nucleus as the appropriate core (residual nucleus) plus two neutrons and one proton. This separation uses fractional parentage coefficients, the squares of which are the total spectroscopic factors.<sup>14</sup> The formulas<sup>15</sup> used to write the target nucleus wave function in this form assumes the removal of a pair of neutrons whose total spins are coupled to zero (i.e., no change of seniority) and, in three of the four cases considered, the removal of an unpaired proton (i.e., change of seniority from 1 to 0). To use the one-step pickup mechanism assumed in the DWBA code, the three extra core nucleons next must be represented as a triton cluster. The transformation required to do this uses Talmi coefficients for both equal<sup>16</sup> and unequal<sup>17</sup> masses.

These Talmi coefficients were formulated in  $l$ - $s$  coupling while the spectroscopic factors were calculated using  $j$ - $j$  coupling; therefore the paired neutron wave function was transformed from  $j$ - $j$  to  $l$ - $s$  coupling assuming the spins and orbital angular momenta are coupled to zero.<sup>18</sup> This method, chosen because of its simplicity, should give reasonable results for the relative reduced widths.

For the case in which  $\text{C}^{12}$  is left in its first excited state, this approximate calculation is no longer valid. The  $1F$  wave function used in the DWBA form factor requires breaking the neutron pair. However, a ratio of reduced widths can be calculated using just the contribution from the  $2P$  wave function for the transitions to the ground and first excited states of  $\text{C}^{12}$ . This

<sup>14</sup> M. H. MacFarlane and J. B. French, *Rev. Mod. Phys.* **32**, 567 (1960).

<sup>15</sup> R. Sherr, in *Proceedings of the Conference on Direct Interactions and Nuclear Reaction Mechanisms, Padua, 1962*, edited by E. Clementel and C. Villi (Gordon and Breach Science Publishers, Inc., New York, 1963), p. 1027.

<sup>16</sup> T. Brody and M. Moshinsky, *Tables of Transformation Brackets for Shell Model Calculations* (Monografias del Instituto de Fisica, Mexico, 1960).

<sup>17</sup> Yu. F. Smirnov, *Nucl. Phys.* **27**, 177 (1961).

<sup>18</sup> M. Rotenberg, R. Bivins, M. Metropolis, and J. Worten, Jr., *The 3-j and 6-j Symbols* (Technology Press, Cambridge, Mass., 1959), p. 22.

TABLE IV. Triton reduced widths.

Target	$ t\rangle$ c.m.	$R_{et}$
$\text{Be}^8\text{g.s.} + (1p_{3/2})^3$	$2p$	0.0412
$\text{C}^{12}\text{g.s.} + (1p_{1/2})^3$	$2p$	0.0412
$\text{C}^{12*} + (1p_{1/2})^2(1p_{3/2})^1$	$2p$	0.103
$\text{O}^{16}\text{g.s.} + (1d_{5/2})^2(2s_{1/2})^1$	$4s$	0.0154
$\text{O}^{16}\text{g.s.} + (2s_{1/2})^3$	$4s$	0.0324

ratio was compared with a calculation<sup>19</sup> using  $l$ - $s$  coupling and found to agree to within 40%.

The dominant shell-model configurations for  $\text{F}^{19}$  were taken to be  $(1d_{5/2})^2(2s_{1/2})$ , and  $(2s_{1/2})^3$  nucleons outside of a closed  $\text{O}^{16}$  ground-state core.<sup>20</sup> These configurations were assumed to have equal probabilities and no coherent effects. The final reduced width for  $\text{F}^{19}$  was the average of the two representations.

The triton reduced widths calculated in this manner are given in Table IV.

For a comparison between extracted and calculated reduced widths, both sets of triton reduced widths were normalized to the  $\text{C}^{12}$  ground state plus triton representation. In this way the relative reduced widths for  $\text{C}^{12}$  first excited and ground states can be directly compared to the calculation using  $l$ - $s$  coupling.<sup>19</sup> These relative widths are given in Table V.

## VI. SUMMARY AND CONCLUSIONS

The three main assumptions made in this investigation are the following: (1) the reaction mechanism is assumed to be direct and the reaction is assumed to proceed by a one-step process, (2) average optical-well parameters based on limited data at a much lower energy are used to describe the  $\text{Li}^7$  elastic scattering, and (3) the reduced widths calculated here are assumed to be a reasonable approximation for the correct triton widths.

TABLE V. Triton relative reduced widths.

Configurations	Form factors	Theoretical relative reduced width	Experimental relative reduced width
$\text{Be}^8\text{g.s.} + t$	$ 2P\rangle$	1	1.79
$\text{C}^{12}\text{g.s.} + t$	$ 2P\rangle$		
$\text{C}^{12*} + t$	$\left\{ \begin{array}{l}  2P\rangle \\  2P\rangle \end{array} \right.$	$2.5(j-j)$	1.22
$\text{C}^{12}\text{g.s.} + t$	$\left\{ \begin{array}{l}  2P\rangle +  1F\rangle \\  2P\rangle \end{array} \right.$	$5(l-s)$	3.67
$\text{O}^{16}\text{g.s.} + t$	$ 4S\rangle$	0.573	2.40
$\text{C}^{12}\text{g.s.} + t$	$ 2P\rangle$		

<sup>19</sup> T. Honda, Y. Kudo, H. Ui, and H. Horie, *Phys. Letters* **10**, 99 (1964).

<sup>20</sup> M. G. Redlick, *Phys. Rev.* **99**, 1421 (1955); **110**, 468 (1958).

A partial justification for assuming a direct one-step pickup process is that the DWBA calculations successfully reproduce the important features of the experimental angular distributions.

A second justification for the assumption of a direct reaction mechanism is the data collected on variations in the differential cross sections with varying  $\alpha$ -particle energies. As was stated in Sec. II, data were taken for all the reactions studied and for selected angles at  $\alpha$ -particle energies 0.6 and 1.2 MeV less than that used for the bulk of the data. The amount of such data collected was necessarily restricted because of the difficulty of obtaining sufficiently intense  $\alpha$  particle beams at these energies. However, what data are available do not show evidence of fluctuations in the cross sections of the magnitude that might be encountered if the reaction mechanism were largely compound-nuclear and such as were observed by Brown *et al.*<sup>4</sup> in the  $(\alpha, \text{Be}^8)$  reaction in the same  $\alpha$ -particle energy range.

The theoretical fits were found not to depend strongly on the particular values of the optical-well parameters chosen; therefore, an average set was used to extract the reduced widths. The absence of any data on the elastic scattering of  $\text{Li}^7$  particles for the energy range appropriate to the reactions reported here makes the DWBA fits calculated somewhat uncertain. The success achieved in using optical-model parameters for the outgoing  $\text{Li}^7$  particles based on elastic scattering data at much lower energies is perhaps an indication of the soundness of the analysis presented here.

Because the  $(\alpha+t)$  system forming  $\text{Li}^7$  is assumed to be in a relative  $1p$  state, the use of zero-range DWBA is not justified. The internal wave function  $\psi(r)$  of  $\text{Li}^7 = \alpha + t$  vanishes at  $r=0$ . Consequently, finite range effects must be considered here. We assume only that

$$\int \phi_t V_{\alpha t} \psi dr = C \phi_t(R_t),$$

where  $C$  is independent of the target and  $\phi_t$  is the wave function of the triton bound in an appropriate level of the potential. This is equivalent to a zero-range approximation for an  $s$  state but can be thought of as including finite-range effects in our case. The actual value of  $C$  will affect the absolute value of any reduced width from the calculation. But as long as  $C$  is the same for all targets, *relative* reduced widths can be extracted without any knowledge of  $C$ .

The justification for using the approximate  $j$ - $j$  coupling calculations is based on the comparison with exact  $l$ - $s$  coupling calculations which was discussed earlier in Sec. V. The relative triton reduced widths calculated in  $j$ - $j$  coupling agreed quite well with these calculated in  $l$ - $s$  coupling.

Bearing in mind the previously described approximations and the justifications of these approximations,

the  $(\alpha, \text{Li}^7)$  reaction would appear to be reasonably well described by a one-step cluster pickup mechanism.

The comparison between the extracted and calculated relative reduced widths in Table V is consistent with the independent-particle-model description of  $\text{B}^{11}$ ,  $\text{N}^{15}$ , and possibly of  $\text{F}^{19}$ . In the latter case there could be some evidence for a small enhancement of triton clustering for the ground state of  $\text{F}^{19}$ . Of course, the theoretical reduced widths depend on the shell-model description of the ground state of  $\text{F}^{19}$ ; however, the configurations chosen should represent an upper limit for these calculated values.

The theoretical description of the ground and first excited states of  $\text{Li}^7$  as an  $\alpha$ -particle plus triton configuration is consistent with the experimental results presented here. That is, after removing the spin factors, the magnitudes of the observed differential cross sections are nearly the same. For the  $\text{B}^{11}$  reactions, the shapes of the angular distributions for the two  $\text{Li}^7$  transitions are almost identical. For the reactions where the angular distributions were out of phase with each other, a spin-orbit interaction could be responsible.<sup>21</sup>

An attempt was made to include the angular dependence arising from the overlap of the  $\text{Li}^7$  and the  $(\alpha+t)$  wave functions using plane-wave theory. The results of including this contribution to the transition amplitude were to improve the over-all PWBA fits to the experimental angular distributions. The use of zero-range DWBA eliminates this angular dependence; therefore, the DWBA fits to the experimental angular distributions might be improved by using finite-range DWBA. Although finite-range DWBA calculations are not expected to alter greatly the shapes of the theoretical angular distributions, relative magnitudes could be altered enough to affect significantly the comparisons of extracted and theoretical reduced widths. This, in turn, would change the interpretation made here about triton clustering in the nuclei studied.

#### ACKNOWLEDGMENTS

The authors would like to express their appreciation to Dr. E. M. Henley for his many valuable comments and suggestions during the latter stages of this investigation.

We also thank the staff of the Nuclear Physics Laboratory, specifically Harold Fauska and his able electronics staff, John Orth for maintaining the accelerator equipment, Joanne Sauer for her assistance in target preparations, Peggy Douglass for her excellent illustrations, Jacque Beechel for operating the cyclotron, and the students, too numerous to mention, for their valuable discussions and help throughout this entire investigation.

<sup>21</sup> E. M. Henley and T. G. Kelley, Phys. Letters 22, 495 (1966).



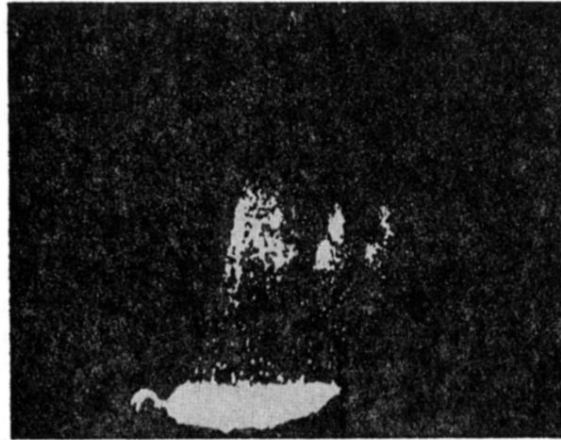


FIG. 1. Photograph showing the multiplier output  $\Delta E(E+k_1\Delta E+k_2)$  along the vertical axis plotted as a function of the total energy  $E+\Delta E$  along the horizontal axis. Lithium ions are in the center of the picture,  $\text{Li}^7$  lying higher than  $\text{Li}^6$ .